RESEARCH ARTICLE

Use of carbonised beet pulp carbon for removal of Remazol Turquoise Blue-G 133 from aqueous solution

Arzu Y. Dursun · Ozlem Tepe · Gülbeyi Dursun

Abstract Carbonised beet pulp (BPC) produced from agricultural solid waste by-product in sugar industry was used as adsorbent for the removal of Remazol Turquoise Blue-G 133 (RTB-G 133) dye in this study. The kinetics and equilibrium of sorption process were investigated with respect to pH, temperature and initial dye concentration. Adsorption studies with real textile wastewater were also performed. The results showed that adsorption was a strongly pH-dependent process, and optimum pH was determined as 1.0. The maximum dye adsorption capacity was obtained as 47.0 mg g^{-1} at the temperature of 25 °C at this pH value. The Freundlich and Langmuir adsorption models were used for describing the adsorption equilibrium data of the dye, and isotherm constants were evaluated depending on sorption temperature. Equilibrium data of RTB-G 133 sorption fitted very well to the Freundlich isotherm. Mass transfer and kinetic models were applied to the experimental data to examine the mechanisms of adsorption and potential rate-controlling steps. It was found that both external mass transfer and intra-particle diffusion played an important role in the adsorption mechanisms of dye and adsorption kinetics followed the pseudo second-order type kinetic model. The thermodynamic analysis indicated that the sorption process was exothermic and spontaneous in nature.

Nomenclature

C	Unadsorbed dye concentration in solution at any time (mg L^{-1})
C_{eq}	Unadsorbed dye concentration in solution at equilibrium (mg L^{-1})
C_0	Initial dye concentration (mg L^{-1})
d_p	Particle diameter (cm)
K_b	Adsorption equilibrium constant (L mg^{-1})
K_F	Freundlich constant
k_L	External mass transfer coefficient (cm min^{-1})
K	Intra-particular diffusion rate constant (mg g^{-1} min$^{-0.5}$)
k_1	Rate constant of pseudo-first order sorption (min^{-1})
k_2	Rate constant of pseudo-second order sorption (g mg^{-1} min^{-1})
n	Freundlich constant
N	Number of data points
q	Adsorbed dye quantity per gram of adsorbent at any time (mg g^{-1})
q_{eq}	Adsorbed dye quantity per gram of adsorbent at equilibrium (mg g^{-1})
q_{max}	Maximum amount of dye per unit weight of the adsorbent to form a complete monolayer on the surface (mg g^{-1})
R	Universal gas constant (8.314 Jmol^{-1} K^{-1})
R^2	Regression correlation coefficient
t	Time (min)

A. Y. Dursun (✉) · O. Tepe
Department of Environmental Engineering, Firat University,
23100 Elazig, Turkey
e-mail: aydursun@firat.edu.tr

G. Dursun
Department of Chemical Engineering, Firat University,
23279 Elazig, Turkey

T Temperature (K, °C)
X Sorbent concentration (g L^{-1})
$\Delta G°$ Gibbs free energy change
$\Delta H°$ Enthalpy change of adsorption
$\Delta S°$ Entropy change of adsorption
SD Normalised standard deviation
ρ_p Particle density (g mL^{-1})

Introduction

Large amounts of dyes are annually produced and used in textile, cosmetics, paper, leather, and other industries. Colour is the first contaminant to be recognised in wastewater. Especially, reactive dyes are the most problematic pollutants compared to other forms of dyes. They are toxic to some aquatic organisms and human beings, cause considerable environmental pollution and must be removed from wastewater completely (Clarke and Anliker 1980; Gupta et al. 2007a,b,c,d,e,f). Many dyes are difficult to decolorise due to their complex aromatic molecular structures and synthetic origin. A range of conventional treatment technologies for dye removal have been investigated extensively. However, most of these methods suffer from one or more limitations, and none of them were successful in completely removing the colour from wastewater (Forgacs et al. 2004; Gupta et al. 2007a,b,c,d,e,f, 2009a,b,c). In this context, adsorption techniques appear as successful efficient alternatives for wastewater treatment (Gupta et al. 1997; Gupta et al. 2002; Ali and Gupta 2007; Gupta et al. 2007a,b,c,d,e,f; Gupta and Ali 2008; Gupta and Rastogi 2008; Gupta and Rastogi 2009, Gupta et al. 2009a,b,c).

Activated carbons are the most common adsorbents in dye adsorption process. They are usually produced from high carbon content materials. Although activated carbons have a good capacity, they suffer from a number of disadvantages. It is quite expensive, and the higher the quality, the greater the cost. (Faria et al. 2004; Hoda et al. 2006). This has led many workers to search for the use of cheap and efficient alternative materials. Some of the materials used with varying success include saw dust, rice husk, peanut shells, cotton seed shell, palm seed coat, apricot stone, almond shell, oak wood waste and cotton stalks and activated sludge process wastes (Malik 2003; Attia et al. 2004; Crini 2006; Gupta et al. 2007a,b,c,d,e,f; Mukherjee et al. 2007; Arslan and Dursun 2008, Gupta et al. 2006a,b,c; Gupta et al. 2010).

Remazol Turquoise Blue-G 133 is one of the most important derivatives of reactive dye class and is preferred due to their brilliant blue, high tinctorial strength, and remarkable chemical stability. It is a copper phthalocyanine reactive dye and consists of a tetrasulfonated copper phthalocyanine with one to two of the sulfonate groups converted to linker arms. Its molecular structure is shown in Fig. 1. While copper phthalocyanine dyes have been used widely in textile industry, little is known about removal of these compounds from wastewaters.

In this study, carbon produced by carbonisation of beet pulp was used as an adsorbent. Beet pulp was chosen considering its large amount availability and the basic cellulosic structure, which is rich of possible binding active sites. Beet pulp carbon obtained from different methods to use as an adsorbent was studied for removing pollutants (Altundogan 2005; Dursun et al. 2005). Aksu and Isoglu (2006, 2007) also made similar studies with Gemazol Turquoise Blue-G dye and investigated adsorption of dye on dried sugar beet pulp. They used beet pulp without making carbonisation process. In the present study, carbon produced from sugar beet pulp at 600 °C in nitrogen atmosphere was used as an adsorbent. It is known that carbonisation process can modify the carbons' physical and chemical properties, influencing their adsorption behaviour and effectiveness. For instance, porosity of adsorbent and the presence and concentration of surface functional groups play an important role in the adsorption capacity and the removal mechanism of the dyes. Therefore, one of the main novelties of the presented manuscript is to show the effect of carbonisation process on sugar beet pulp and determines the difference in dye adsorption capacities and yields between dried sugar beet pulp and carbonised sugar beet pulp. In literature, the studies focusing on dye adsorption on beet pulp carbon and application of beet pulp carbon to the real textile wastewater are very limited, and there is still lack of works on evaluating equilibrium, kinetic and thermodynamic parameters of
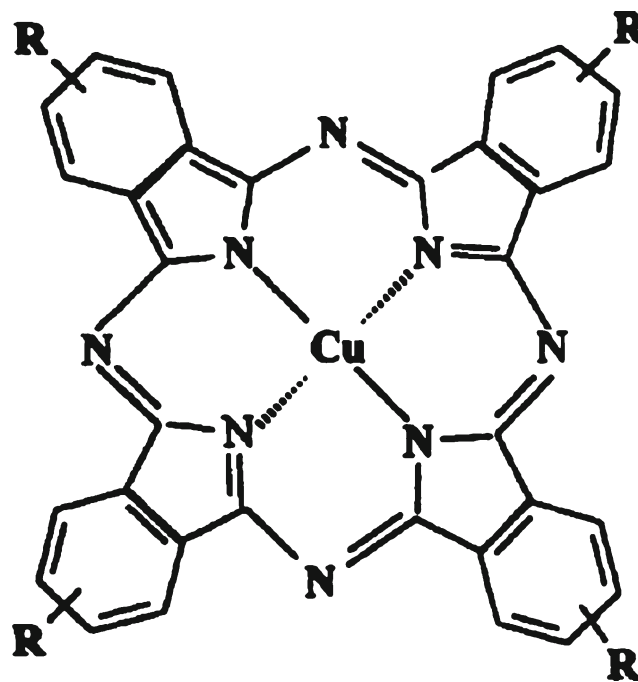

Fig. 1 Molecular structures of RTB-G 133 dye

the process, which are important in the design of treatment processes The objective of this study was to produce beet pulp carbon (BPC) as an adsorbent for adsorption of Remazol Turquoise Blue-G 133 dye (RTB-G 133), to characterise it and to investigate the effects of initial dye concentration, contact time, temperature and pH. Equilibrium isotherm data were fitted to Langmuir and Freundlich equations, and constants of isotherm equations were determined. The mechanisms of RTB-G 133 dye sorption onto BPC and potential rate-controlling steps were examined using external mass transfer and intra-particle diffusion models. Furthermore, pseudo-first- and second-order kinetic models were also used to analyse adsorption kinetics. Finally, thermodynamic parameters were evaluated using adsorption data, and adsorption studies with real textile wastewater were performed.

Adsorption equilibrium

Equilibrium study on adsorption has provided information on the capacity of the adsorbent. In addition, an adsorption isotherm is characterised by certain constant values that express the surface properties and affinity of the adsorbent and can also be used to compare the adsorptive capacity of the adsorbent for different pollutants. The Langmuir model is valid for monolayer adsorption onto a surface with a finite number of identical sites, which are homogeneously distributed over the adsorbent surface. It is given by Eq. 1 (Smith 1981).

$$q_{eq} = \frac{q_{max} K_b C_{eq}}{1 + K_b C_{eq}} \qquad (1)$$

where q_{eq} is the dye adsorbed on carbon at equilibrium, C_{eq} is the equilibrium concentration in the solution, q_{max} is the adsorption capacity and K_b is the adsorption equilibrium constant related to energy of adsorption. The Freundlich model is however an empirical equation based on adsorption on a heterogeneous surface, suggesting that binding sites are not equivalent and/or independent. Freundlich equation is expressed as:

$$q_{eq} = K_F C_{eq}^{1/n} \qquad (2)$$

where K_F and n are indicators of the adsorption capacity and intensity, respectively (Smith, 1981).

Adsorption kinetics

Sorption kinetics shows a large dependence on the physical and/or chemical characteristics of the sorbent material, which also influences the sorption mechanism. Adsorption kinetics of RTB-G 133 dye onto BPC is mainly controlled by three consecutive steps including diffusion processes (Findon et al. 1993): adsorbate (dye) transport from the boundary film to the surface of the sorbent (film diffusion), transfer of adsorbate from the surface to the intra-particular

active sites (intra-particular diffusion), and uptake of adsorbate by the active sites on the surface of the adsorbent. The last step is considered to be an equilibrium reaction and assumed to be rapid while the other steps are the rate determining steps, either singly or in combination.

External mass transfer model

External mass transfer is characterised by the initial rate of solute diffusion for the system studied. According to the boundary model, change in the dye concentration with respect to time can be written as follows (McKay 1983; Findon et al. 1993).

$$\frac{dC}{dt} = -k_L S(C - C_s) \qquad (3)$$

where C is the liquid phase solute concentration of dye at a time t, C_S is the liquid phase solute concentration at the particle surface, k_L is the liquid–solid mass transfer coefficient (external mass transfer coefficient) and S is the specific surface area for mass transfer. It is assumed that during the initial stages of adsorption, the intra-particle resistance is negligible and the transport is mainly due to film diffusion mechanism. At $t=0$, the surface concentration of dye, C_S, is negligible and $C=C_0$. With these assumptions, Eq. 3 can be simplified as:

$$\frac{d(C/C_O)}{dt} = -k_L S \qquad (4)$$

Assuming the adsorbent particles are spherical, S is calculated from Eq. 5:

$$S = \frac{6X}{d_p \rho_p} \qquad (5)$$

where X is the sorbent concentration in the solution, d_p is the average particle diameter and ρ_p is the density of the sorbent. By plotting C/C_0 against t, the value of k_L may be determined from the slope at $t=0$.

Intra-particular mass transfer diffusion model

In order to gain insight into the mechanisms and rate controlling steps affecting the kinetics of adsorption, the kinetic experimental results were fitted to the intra-particle diffusion model (Weber and Morris 1963).

$$q = f\left(\frac{Dt}{r_P^2}\right)^{0.5} = Kt^{0.5} \qquad (6)$$

where r_p is the particle radius, D the effective diffusivity of solutes within the particle, and K is the intra-particular diffusion constant. Such types of plots may present multi-linearity, implying that the overall adsorption process may be controlled by one or more steps, such as film or external diffusion, intra-particle diffusion and a chemical reaction on

the pore surface, or a combination of more than one step. Weber and Morris (1963) reported that if intra-particle diffusion was involved in the adsorption process, then a plot of the square root of time versus the adsorption amount would result in a linear relationship and that the intra-particle diffusion would be the only rate-controlling step if this line passes through the origin. Otherwise, some other mechanisms along with intra-particle diffusion are also involved. K values can be determined by linearising the curve $q=f(t^{0.5})$.

Pseudo-first-order kinetic model

Lagergren's model (1898) is the most widely used rate equation in liquid phase sorption and is expressed as:

$$\frac{dq}{dt} = k_1 \left(q_{eq} - q \right) \tag{7}$$

where q is adsorbed dye quantity per gram of sorbent at any time, and k_1 is the rate constant of pseudo-first-order sorption. The integrated form of the Eq. 7 for the boundary conditions $t=0$ to $t=t$ and $q=0$ to $q=q$ was given in Eq. 8. The kinetic constant k_1 can be determined by plotting log $(q_{eq}-q)$ against of t.

$$\log\left(q_{eq} - q\right) = \log\left(q_{eq}\right) - \frac{k_1}{2,303} t \tag{8}$$

Pseudo-second-order model

Ho and McKay (1999) developed a second-order equation based on adsorption capacity. This kinetic model can be written as:

$$\frac{dq}{dt} = k_2 \left(q_{eq} - q \right)^2 \tag{9}$$

Integrating the above equation for the boundary conditions $t=0$ to $t=t$ and $q=0$ to $q=q$ gives:

$$\frac{t}{q} = \frac{1}{k_2 q_{eq}^2} + \frac{1}{q_{eq}} t \tag{10}$$

where k_2 is the rate constant of pseudo-second-order sorption The q_{eq} and k_2 can be determined from the slope and intercept of the plot.

The normalised standard deviations for pseudo-first-order and pseudo-second-order models were evaluated using Eq. 11.

$$SD(\%) = 100 \sqrt{\frac{\sum \left(\left(q_{t,exp} - q_{t,cal} \right) / q_{t,exp} \right)^2}{N-1}} \tag{11}$$

where the subscripts 'exp' and 'cal' show the experimental and calculated values, respectively, and N is the number of data points (Wu et al. 2009).

Thermodynamic parameters of adsorption

The thermodynamic parameters, namely free energy ($\Delta G°$), enthalpy ($\Delta H°$) and entropy changes ($\Delta S°$), have an important role to determine spontaneity and heat change for the adsorption process. The free energy change of the adsorption is given by the following equation:

$$\Delta G° = -RT \ln K \tag{12}$$

where R is the universal gas constant and T is the absolute temperature (K), and K_b is the equilibrium constant (the Langmuir constant). Equilibrium constant can be used in the Van't Hoff equation to evaluate the thermodynamic parameters as a function of temperature. The equation is given as (Smith and Van Ness 1987):

$$\ln K_b = \frac{\Delta S°}{R} - \frac{\Delta H°}{RT} \tag{13}$$

The enthalpy and entropy changes of the process can be determined from the slope and intercept of line obtained by plotting $\ln K_b$ versus $1/T$.

Materials and methods

Preparation of beet pulp carbon

In this study, the waste pulp of sugar beet remaining from extraction of sugar was used to produce carbon. The pulp was obtained from the sugar factory in Elazığ, Turkey. The collected material was washed and dried at oven at 105 °C for 1 day. It was grounded and sieved to 50–100 mesh size (0.34–0.15 mm). Then, powder of beet pulp (25 g) was placed in a horizontal ceramic tube furnace and heated up to 600 °C at a rate of 5 °C/min. In the meantime, nitrogen was fed into the oven by a rate of 1 L/min. It was left at this temperature to thermally decompose to porous carbonaceous materials for 1 1/2 h and then allowed to cool to room temperature in nitrogen atmosphere. Carbon production yield from beet pulp was 25 %. The carbon was grounded and screened through different mesh size and stored in a closed bottle to be used in adsorption studies.

The surface area of BPC measured using Micromeritics FlowSorb II-2300 was obtained by using N_2 adsorption. To determine adsorption characteristic of BPC, the iodine number was also measured.

Chemicals

Remazol Turquoise Blue-G 133 dye was kindly supplied from Gemsan, Turkey and used without further purification (colour index name, Reactive Blue 21; molecular weight= 576.1 gmol^{-1}). Stock solution was prepared by dissolving

1.0 g of dye in 1 L of double-distilled water. The test solutions were prepared by diluting of stock solution to the desired concentrations. The range of concentrations of prepared dye solutions changed between 20 and 500 mg L^{-1}. The pH of each solution was adjusted to the required value with diluted or concentrated H_2SO_4 and NaOH solutions before contacting the sorbent. The preliminary studies showed that the initial pH value did not change considerably during the experimental period.

Adsorption studies

This method involved agitating (150 rpm) Erlenmeyer flasks of 0.25 L containing 0.15 g BPC 0.15 L of RTB-G 133 dye solutions at the desired concentration, temperature and pH. Samples of 5 mL were taken from mixture during stirring at pre-determined time intervals for determining the residual colour concentration in the medium. Before analysis, samples were centrifuged at 5,000 rpm for 5 min, and supernatant liquid was analysed for the remaining colour. All the experiments were carried out in duplicates, and average values were used for further calculations.

Analysis

The concentration of unadsorbed RTB-G 133 dye in the adsorption medium was measured colorimetrically (Jenway 6105 UV/Vis spectrophotometer). The absorbance of the colour was read at 580 nm, where the maximum absorption peak existed. All the instruments used in experiments were provided from Laboratories' of F.U. Environ. Eng. Dept.

The Brunauer–Emmett–Teller (BET) surface area was determined using a Micromeritics FlowSorb II-2300 surface area analyser. To determine adsorption characteristic of BPC, the iodine number (IN) of carbon was determined by shaking 0.5 g of each sample with 100 cm^3 aqueous solution of iodine (2.7 g $I_2 dm^{-3}$) at 25 °C. The gram amount of iodine adsorbed per gram carbon was taken as iodine number. The infrared spectrum of BPC was obtained with a Mattson 1000 FTIR spectrometer.

Results and discussion

Surface area and iodine number are important characteristics, capable of affecting the quality and utility of adsorbents. For this reason, it is important to determine and control them accurately. The BET surface area of the BPC was determined as 47.5 $m^2 g^{-1}$. Other properties of the BPC were measured as iodine number 270 mg $I_2 g^{-1}$ and bulk density 0.576 $g cm^{-3}$.

Adsorption data for the uptake of RTB-G 133 dye onto BPC was investigated at various initial concentration, temperature and pH. The results are given as the units of adsorbed
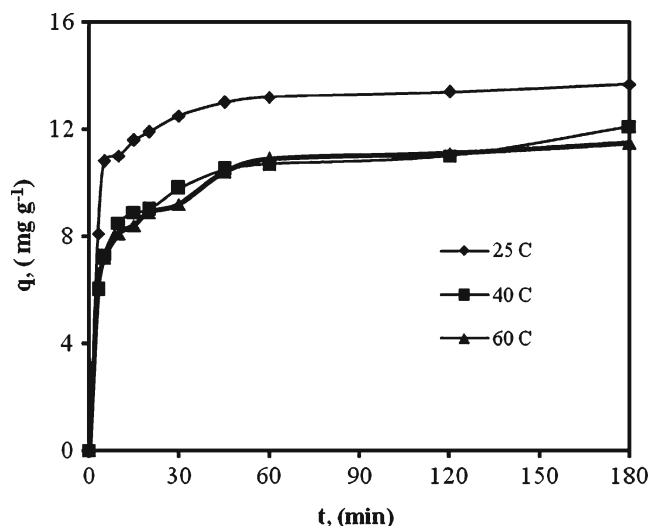

Fig. 2 The adsorption curves of RTB-G 133 dye ($C_0 = 40$ mg L^{-1}, pH=1.0, $X = 1.0$ g L^{-1}, agitation rate=150 rpm)

RTB-G 133 dye quantity per gram of adsorbent at any time (q) and at equilibrium (q_{eq}), unadsorbed RTB-G 133 dye concentration in solution at any time (C) and at equilibrium (C_{eq}). Adsorption yield is given as: [Ads. %=100 ($C_0 - C_{eq})/C_0$]. Adsorption capacity is given as: [$q = (C_0 - C)/X$].

Effect of contact time

Adsorption kinetics studies were carried out to understand the dye adsorption behavior of the sorbent with respect to time, concentration and temperature. Figure 2 presents the adsorption kinetics of RTB-G 133 dye at 25, 40 and 60 °C by plotting the dye uptake capacity versus time. As seen, the extent of dye removal increased with increasing contact time linearly at the beginning showing a rapid uptake of dye ions,
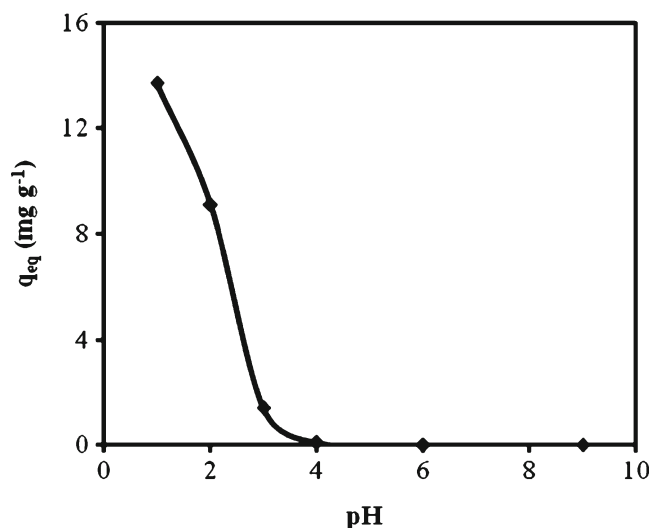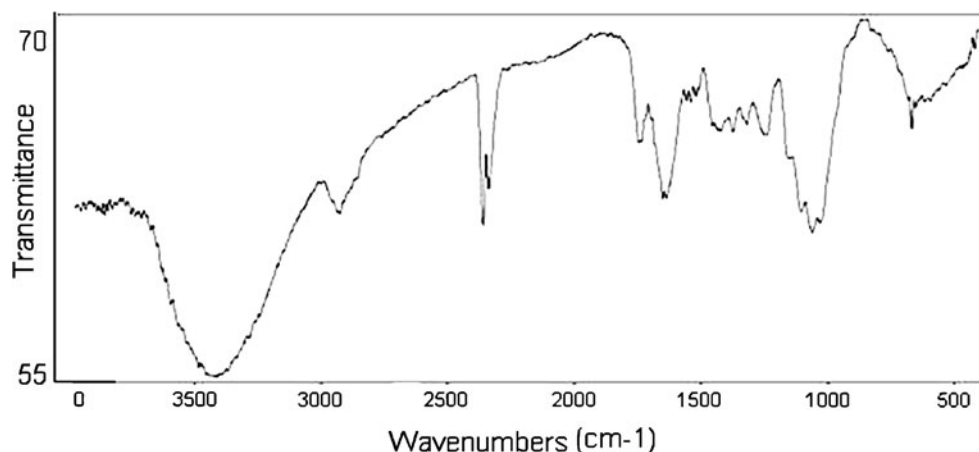

Fig. 3 Effect of pH on the RTB-G 133 dye adsorption ($C_0 = 40$ mg L^{-1}, $T = 25$ °C, $X = 1.0$ g L^{-1}, agitation rate=150 rpm)

then non-linearly at a slower rate and finally attained saturation called the equilibrium time. At initial stage, the driving force is higher, which permits to overcome all the external mass transfer resistances and the active sites with higher affinity are first occupied. Dye concentration in solution then decreases, decreasing the driving force, and the remaining active sites with lower affinities are occupied slowly. Adsorption studies were carried out for 24 h (data were given for 3 h), and it was observed that the adsorption capacity decreased with increasing temperature. A larger amount of dye was removed in the first 30 min of contact time. Equilibrium was established in 60 min at the end of a rapid adsorption for all the temperatures studied, and after that, no more RTB-G 133 dye was adsorbed.

Effect of pH on adsorption

Figure 3 presents the variation of equilibrium dye uptake with initial pH for 40 (mg L^{-1}) initial dye concentration. Experiments were carried out over a pH range of 1.0–10.0, and the highest uptake value was found as 13.7 (mg g^{-1}) at pH 1.0. The adsorption of dye decreased significantly with increase in pH, so further adsorption experiments were performed at this pH value. Solution pH affects both aqueous chemistry and surface binding sites of the adsorbents.

Couglin and Ezra (1968) reported that oxidised carbons had mainly carbonyl, hydroxyl and a very small quantity of carbonyl groups. Acid treatment produces more active acidic surface groups such as carboxyl and lactone, resulting in an increase in the adsorption of anionic dyes. Figure 4 shows the IR spectrum of BPC. As seen from the figure, BPC contains several functional groups such as hydroxyl peak at 3,408 cm^{-1}, carbonyl peak at 2,925 cm^{-1} and asymmetric carboxylate peak at 1,630 cm^{-1}. Since the dye species carry negative charge due to sulfonate groups, electrostatic attractions are expected to have a considerable contribution to the overall interactions. Depending on pH, functional groups of the adsorbent may change their valances. It is expected that at pH 1.0, most of the potential fixation sites on BPC are protonated, and the surface of sorbents are surrounded by hydronium ions. Reactive dyes are known to ionise to a high degree in aqueous solutions to form colored anions due to the sulfonate group(s) in their structures. Sulphonate ($-SO_3-$) groups of RTB-G 133 dye are easily dissociated and have negative charges in the aquatic environment. The higher uptakes obtained at very acidic pH could be attributed to the electrostatic interactions between the positively charged sorbent and the negatively charged dye anions. As the pH of the system increases, the number of negatively charged sites increases and the number of positively charged sites

Table 1 The equilibrium uptake capacities and adsorption yields obtained at different initial concentrations and temperatures

C_o (mg L^{-1})	25 °C		40 °C		60 °C	
	q_{eq} (mg g^{-1})	Adsorption (%)	q_{eq} (mg g^{-1})	Adsorption (%)	q_{eq} (mg g^{-1})	Adsorption (%)
20	9.9	49.5	7.7	38.5	7.3	36.5
40	13.7	34.3	12.1	30.3	11.5	28.8
75	20.9	27.9	16.5	22.0	16.0	21.3
100	25.8	25.8	19.6	19.6	17.3	17.3
250	34.0	13.6	28.0	11.2	24.0	9.6
500	47.0	9.4	39.0	7.8	37.0	7.4

decreases. A negatively charged surface site on the adsorbent does not favour the adsorption of dye anions due to the electrostatic repulsion.

Effect of initial RTB-G 133 dye concentration on temperature depended adsorption

The effect of temperature on RTB-G 133 dye sorption capacity of BPC was investigated in the temperature range of 25–60 °C at varying initial dye concentrations. The results show that maximum adsorption capacity values were obtained at 25 °C for all initial dye concentrations and uptake capacity of BPC decreased from 47.0 to 37.0 mg g^{-1} with increasing the temperature from 25 to 60 °C at 500 mg L^{-1} initial dye concentration. These results pointed that adsorption of RTB-G 133 dye by BPC has an exothermic character. Since sorption is an exothermic process, this is an expected result due to weakened physical bonding between the dye and active sites of the adsorbents with increasing temperature.

Table 1 also shows the effect of initial dye concentration on the sorption capacity of BPC. As a rule, increasing the initial dye concentration results in an increase in the adsorption capacity because the initial dye concentration provides a driving force to overcome mass transfer resistances between the adsorbent and adsorption medium. Therefore, higher adsorption capacities were obtained at higher initial concentrations at all temperatures studied. The adsorption yields determined at different initial dye concentrations were also compared in Table 1. At lower concentrations, all sorbate ions present in the adsorption medium could interact with the binding sites so higher adsorption yields were obtained. At higher concentrations, lower adsorption yield were observed because of the saturation of the adsorption sites. Therefore, increasing dye concentration generally caused a decrease in the adsorption yield. The maximum adsorption yields were determined as 49.5, 38.5 and 36.5 % at 20 mg L^{-1} initial dye concentration for 25, 40 and 60 °C, respectively. The adsorption yields were also influenced by temperature and decreased with increasing temperature. The decrease in the adsorption yield and adsorption capacity at increased temperature indicated that the sorption of RTB-G 133 dye onto BPC is exothermic in nature.

Aksu and Isoglu (2006) made similar study with Gemazol Turquoise Blue-G dye and investigated adsorption of dye on dried sugar beet pulp. They used beet pulp without making carbonisation process. The highest Gemazol Turquoise Blue-G dye uptake capacity was determined as 234.8 mg g^{-1} at 25 °C, pH=2, 800 mg L^{-1} initial dye concentration. Simultaneous biosorption of Gemazol Turquoise Blue-G dye and copper (II) cations to dried sugar beet pulp, from binary mixtures was studied by Aksu and Isoglu (2007). The
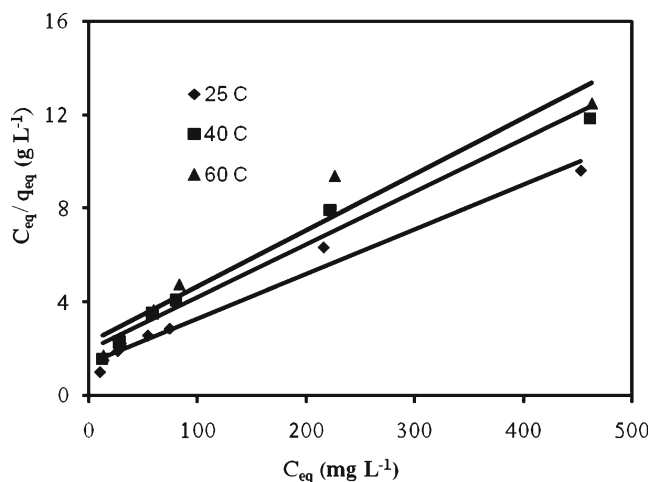

Fig. 5 The linearised Langmuir adsorption isotherm of RTB-G 133 dye

equilibrium uptake of each component increased with increasing its initial concentration up to 750 mg L^{-1} for dye and up to 200 mg L^{-1} for copper (II) ions. Kargi and Ozmıhcı (2005) compared adsorption performances of powdered activated sludge and powdered activated carbon for removal of Turquoise Blue dyestuff. More than 95 % dyestuff removal efficiencies were obtained for both adsorbent at the end of 6 h with adsorbent concentrations above 4 gL^{-1}. Özer and Dursun (2007) presented the methylene blue adsorption capacity of dehydrated wheat bran (BET surface area=9.5 m^2 g^{-1}) as 99.84 mg g^{-1} for initial methylene blue concentration of 200 mg L^{-1} at 45 °C. Ferrero (2007) studied with hazelnut shell for removal of Acid blue 25. The maximum uptake of dye was found to be 60.2 mg g^{-1} at the pH=4.5. Mittal et al. (2010) investigated adsorption of Chrysoidine Y on bottom ash and de-oiled soya. The dye sorption capacities of bottom ash and de-oiled soya were
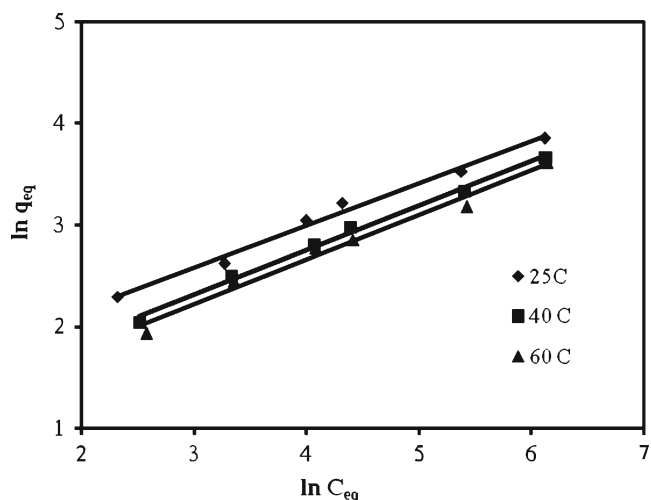

Fig. 6 The linearised Freundlich adsorption isotherm of RTB-G 133 dye

Table 2 Isotherms constants for RTB-G 133 dye adsorbed on BPC

T (°C)	Langmuir model			Freundlich model		
	q_{max} (mg g^{-1})	K_b (L mg^{-1})	R^2	K_F [(mg g^{-1})(mg L^{-1})^n]	n	R^2
25	52.63	0.0134	0.9775	3.83	2.42	0.9888
40	44.64	0.0112	0.9755	2.73	2.29	0.9943
60	41.67	0.0105	0.9460	2.45	2.27	0.9809

determined as 3.61×10^{-5} and 1.92×10^{-5} mol g^{-1} at 30 °C, respectively. Jain et al. (2010) removed hazardous dye Naphthol Yellow S from wastewater using activated carbon and activated de-oiled mustard. Amounts of adsorbed adsorbate were determined as approximately 8.0×10^{-5} mol L^{-1} and 7.0×10^{-5} mol L^{-1} for 0.5 gL^{-1} activated carbon and 4 gL^{-1} activated de-oiled mustard, respectively. The wheat husk, an agricultural by-product, has been activated and used as an adsorbent for the adsorption of Reactofix golden yellow 3 RFN from aqueous solution by Gupta et al. (2007a, b, c, d, e, f). Maximum adsorption capacity was reported as 0.1158 mmol/g. Removal of erythrosine was carried out using waste material—hen feathers—as adsorbent. The effects of pH, concentration of the dye, temperature and adsorbent dosage have been studied. Adsorption capacity for pH 8.39 was found extremely low, and when pH decreased from 4.00 to 2.00, adsorption capacity increased by twofold Gupta et al. (2006a, b, c). Carbon slurry was used as adsorbent for the removal of two reactive dyes from synthetic textile wastewater. Dye adsorption capacities of the adsorbent for the Vertigo Blue 49 and the Orange DNA13 were 11.57 and 4.54 mg g^{-1} adsorbent, respectively (Gupta et al. 2007a,b,c,d,e,f). An azo dye, Acid Orange 7 was removed by adsorption over two waste materials, namely bottom ash and de-oiled soya. Maximum adsorption yields for bottom ash and de-oiled soya were reported as 78 and 80 % at 3×10^{-5} M initial dye concentration (Gupta et al. 2006a,b,c). It is obvious that the maximum uptake values of RTB-G 133 dye found in this work (47.0 mg g^{-1}) is reasonably better than some of the results given in the literature.

Determination of equilibrium parameters

Equilibrium data, commonly known as adsorption isotherms, are basic requirements for the design of adsorption systems. The sorption constants calculated according to the Langmuir and the Freundlich sorption models at different temperatures. Initial dye concentrations were varied from 20 to 500 mg L^{-1}, while the adsorbent concentration was kept constant (1.0 gL^{-1}). The linearised isotherms are presented in Figs. 5 and 6. The isotherm constants and correlation coefficients are tabulated in Table 2. In view of these values, the isotherms appeared to follow the Freundlich model more closely than the Langmuir model. The maximum capacity q_{max} determined from the Langmuir isotherm defines the adsorption capacity when the surface is fully covered with dye. The adsorption capacity of the adsorbent decreased with increasing the temperature and maximum q_{max} values were determined as 52.63 mg g^{-1} at 25 °C. A high K_b value indicates the affinity for binding dye. When the adsorption is exothermic, an increase in T results in a decrease in K_b. The highest value of K_b was found as 0.0134 at 25 °C. The Freundlich equation is based on a monolayer adsorption by the adsorbent with a heterogeneous energy distribution of active sites. The surface of the biological materials was expected to have heterogeneous energies for adsorption, so a good fit was obtained. The values of Freundlich constants decreased with increasing temperature and the highest K_F value was reported as 3.83 mg g^{-1} at 25 °C. All n values were found high enough for adsorption (>1.0).

Table 3 Effect of initial RTB-G 133 dye concentration and temperature on the external mass transfer coefficients (k_L) and intra-particle diffusion rate constants (K)

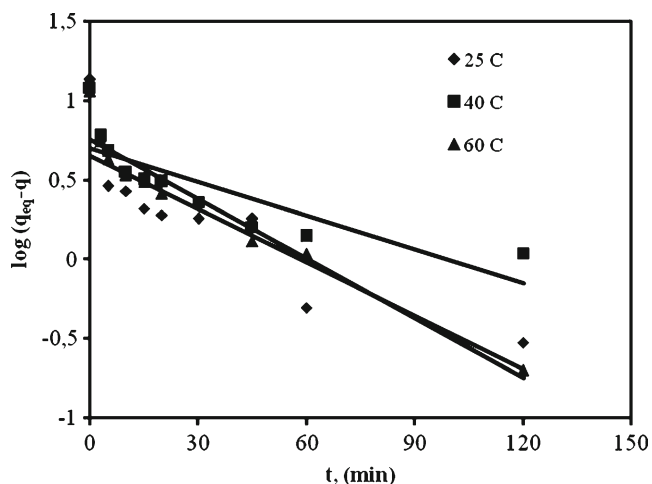| C_0 (mg L^{-1})	25 (°C)		40 (°C)		60 (°C)	
	k_L (cm min^{-1})	K (mg g^{-1} min$^{-0.5}$)	k_L (cm min^{-1})	K (mg g^{-1} min$^{-0.5}$)	k_L (cm min^{-1})	K (mg g^{-1} min$^{-0.5}$)
20	0.332353	0.7472	0.196078	0.2748	0.147059	0.2023
40	0.220588	1.3659	0.166111	1.2857	0.117647	0.7340
75	0.212056	1.4758	0.161209	1.4210	0.097603	1.0652
100	0.206971	1.5270	0.152516	1.4449	0.091503	1.1757
250	0.108922	2.6694	0.091503	1.5232	0.078431	1.2148
500	0.076242	3.0636	0.065359	1.7664	0.062092	1.3935

Fig. 7 Pseudo-first-order adsorption kinetics of RTB-G 133 dye at different temperatures

Kinetic parameters of adsorption

In order to gain insight into the mechanisms and rate controlling steps affecting the kinetics of adsorption, the kinetic experimental results were fitted to the kinetic models. In the first step of adsorption, the film diffusion (external mass transfer) is an important rate-controlling step and is characterised by the initial rate of solute diffusion for the system studied. The effect of initial dye concentration on the external diffusion rate was given by a plot of C/C_o versus time for 20 and 500 mg L^{-1} initial dye concentrations (data not shown). It was reported that the concentration of RTB-G 133 dye falls very fast during the initial uptake before intra-particular diffusion could begin to control the adsorption kinetics for all cases. All the kinetic data were fitted to Eq. 4 for the initial uptake phase and the external mass transfer coefficients were presented in Table 3. The results showed that the increase in initial dye concentration resulted in a decrease in the external mass transfer coefficient and external mass transfer. It was also indicated that the values of external mass transfer coefficient decreased with increasing temperature. It is clear that, as expected, external mass transfer cannot be neglected, although this resistance is only significant for the initial period of adsorption time.

The plots of Q against the $t^{0.5}$ at all initial dye concentrations and at 25, 40 and 60 °C temperatures (data not shown) revealed that all the plots have the same general

feature presenting multi-linearity, indicating that a few steps took place. The first, sharper portion obtained in the very beginning period, which extent is related to initial dye concentration and temperature, is attributed to the diffusion of adsorbate through the solution to the external surface of adsorbent or the boundary layer diffusion of solute molecules. The second linear portion describes the gradual layer adsorption stage, where intra-particle diffusion is rate limiting. The third portion is attributed to the final equilibrium stage for which the intra-particle diffusion started to slow down due to the low dye concentration left in the solution. The linear plots of second portion at each concentration and temperature did not pass through the origin; this is indicative of some degree of boundary layer control, and this shows further that the intra-particle diffusion is not only rate-controlling step. The intra-particle rate constant at different initial concentrations obtained from the slope of the plots was summarised in Table 3. As seen from the table, the rate of diffusion increased with a raise in initial dye concentration and decreased with increasing temperature of solution. This may be due to a greater driving force with increasing dye concentration. Increasing the dye concentration in the solution promoted the diffusion in the particles.

The plots of linearised form of the pseudo-first order equation are shown in Fig. 7. The values of k_1, q_{eq} and correlation coefficients are compared in Table 4. The results showed that the correlation coefficient for the first-order kinetic model obtained at 25 °C was low, and the theoretical $q_{eq,cal}$ values found from this model did not give reasonable values, so the pseudo-first-order model did not describe the adsorption results of dye onto BPC.

Using Eq. 11, t/q was plotted against t, and second-order adsorption rate constant ($k_{2,ad}$) and equilibrium uptake values (q_{eq}) were determined from the slope and intercept of the plots (Fig. 8). The values of the parameters $k_{2,ad}$ and q_{eq} and of correlation coefficients are also presented in Tables 4. As seen from the table, the values of correlation coefficient were very high, and the theoretical q_{eq} values were much closed to the experimental q_{eq} values. Furthermore, in order to quantitatively compare the applicability of each model, a normalised standard deviation was evaluated using Eq. 11, and the normalised standard deviation value for pseudo-first-order model (SD=72.28) was found to be lower than the pseudo-second-order kinetic model's (SD=1.89). In the view of

Table 4 Change of the pseudo-first- and second-order reaction rate constants with temperature

T (°C)	$q_{eq,exp}$ (mg g^{-1})	First-order kinetic model			Second-order kinetic model		
		k_1 (min^{-1})	$q_{eq, cal}$ (mg g^{-1})	R^2	k_2 (g mg^{-1} min^{-1})	$q_{eq,cal}$ (mg g^{-1})	R^2
25	13.70	0.02602	4.49	0.772	0.021383	13.85	0.999
40	12.10	0.01635	5.06	0.692	0.014414	12.12	0.997
60	11.50	0.02878	5.70	0.935	0.015146	11.78	0.999
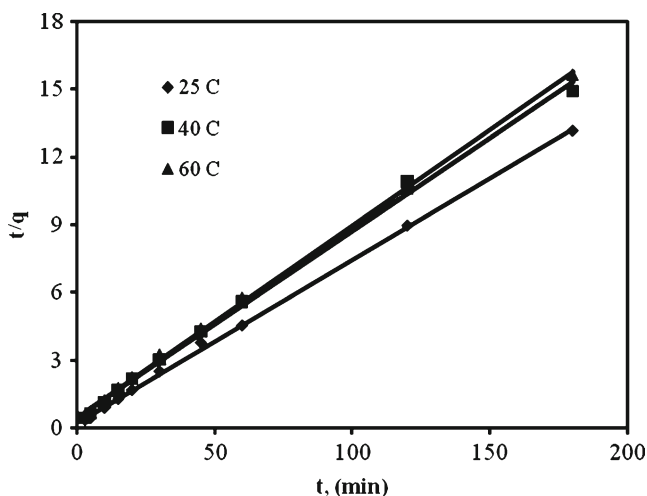
Fig. 8 Pseudo-second-order adsorption kinetics of RTB-G 133 dye at different temperatures

Fig. 9 $\ln K_b$ vs. $1/T$ plot

these results, it can be said that the pseudo-second-order kinetic model in contrast to the pseudo-first-order model provided a good correlation for the adsorption. The theoretical q_{eq} values also agreed very well with the experimental q_{eq} values in the case of pseudo-second-order kinetics. These results suggest that the sorption process may be best described by the pseudo-second-order with external mass transfer and intra-particle diffusion as one of the rate determining steps.

Thermodynamic parameters of adsorption

The thermodynamic parameters reflect the feasibility and spontaneous nature of the process. Table 5 presents The Gibbs free energy change values for the adsorption process. All the Gibbs free energy change values are negative. A negative value of $\Delta G°$ indicates the feasibility of the process and spontaneous nature of the adsorption. The standard enthalpy change of the adsorption determined from the $\ln K_b$ versus $1/T$ plot (Fig. 9) was -5.556 kJ mol^{-1}. The negative value of $\Delta H°$ suggests the exothermic nature of adsorption. The entropy change of the adsorption at 25 °C was determined as 0.056 kJ mol^{-1} K^{-1}, and the positive value of $\Delta S°$ confirms the increased randomness at the solid–solution interface during adsorption.
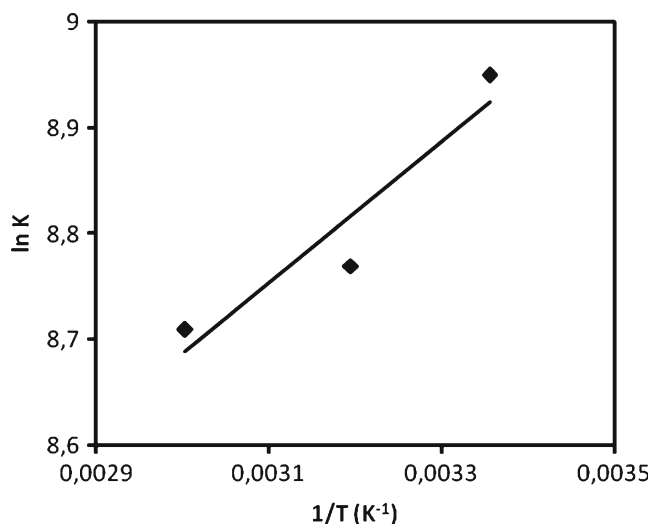
Application to real wastewater

In order to investigate the potential performance of BPC in real textile effluents, experiments were performed using real textile wastewater containing RTB-G 133 dye under optimised conditions (pH 1.0; adsorbent dosage, 1.0 gL^{-1}; volume of wastewater, 100 mL). The initial RTB-G 133 concentration and COD value of the wastewater were 2,914 and 7,000 mg L^{-1}, respectively, while its initial pH value was 12.3. After a 5-h adsorption process, concentrations of RTB-G 133 and COD value were determined as 2,706 and 4,500 mg L^{-1}, respectively. Based on these results, 35.7 % COD and 7.14 % dye removal were obtained in case of real wastewater effluent under the same optimised conditions. The results indicated that in industrial wastewater, the adsorption capacity of sorbent was decreased due to the presence of interfering species in the wastewater.

Conclusion

Dyestuff removal performance of BPC was tested at initial pH, different dye concentrations and temperatures. It was found that sorption was strongly pH dependent, and optimum pH was determined as 1.0. It is also reported that dye adsorption decreased with increasing temperature. The Langmuir and Freundlich adsorption isotherms were used to correlate the equilibrium adsorption data, and the isotherm constants were determined. The Freundlich isotherm provided a better fit than the other. A film diffusion model and an intra-particle diffusion model developed by Weber and Morris (1963) were used to find both the boundary and intra-particle diffusion rate constants. The sorption data indicated that the mechanism of dye adsorption by BPC is

Table 5 $\Delta G°$ values for adsorption of RTB-G 133 dye at different temperatures	T (°C)	K_b (L mg^{-1})	$-\Delta G°$ (kJ mol^{-1})
	25	0.0134	22.18
	40	0.0112	22.82
	60	0.0105	24.11

rather complex and is probably a combination of external mass transfer, intra-particle diffusion and sorption process. The suitability of the pseudo-first- and pseudo-second-order kinetic models was also used to test adsorption kinetics. It was shown that the adsorption of RTB-G 133 dye on to BPC could be best fitted to the pseudo-second-order model. Thermodynamic constants were also evaluated using equilibrium constants changing with temperature. The negative value of $\Delta G°$ indicated the spontaneity, and the negative values of $\Delta H°$ showed the exothermic nature of adsorption. When the proposed adsorption system was applied to real effluent, 35.7 % COD and 7.14 % dye removal were obtained under the same optimised conditions.

References

Aksu Z, Isoglu IA (2006) Use of agricultural waste sugar beet pulp for the removal of gemazol turquoise blue-G reactive dye from aqueous solution. J Hazard Mater B137:418–430

Aksu Z, Isoglu IA (2007) Use of dried sugar beet pulp for binary biosorption of Gemazol Turquoise Blue-G reactive dye and copper (II) ions: equilibrium modelling. Chem Eng J 127:177–188

Ali I, Gupta VK (2007) Advances in water treatment by adsorption technology. Nature Protocols 1:2661–2667

Altundogan HS (2005) Cr (VI) removal from aqueous solution by iron (III) hydroxide-loaded sugar beet pulp. Process Biochem 40:1443–1452

Arslan ÇS, Dursun AY (2008) Biosorption of phenol on dried activated sludge: effect of temperature. Sep Sci and Technol 43:3251–3268

Attia AA, El-Hendawy ANA, Khedr SA, El-Nabarawy T (2004) Textural properties and adsorption of dyes onto carbons derived from cotton stalks. Adsorpt Sci and Tech 22:411–426

Clarke EA, Anliker R (1980) Organic dyes and pigments. The handbook of environmental chemistry. 3. Part A. Anthropogenic compounds. Springer, New York

Couglin RW, Ezra FS (1968) Role of surface acidity in the adsorption of organic pollutants on the surface of carbon. Environ Sci Technol 2:291–297

Crini G (2006) Non-conventional low-cost adsorbents for dye removal: a review. Bioresour Technol 97:1061–1085

Dursun G, Çiçek H, Dursun AY (2005) Adsorption of phenol from aqueous solution by using carbonized beet pulp. J Hazard Mater B125:175–182

Faria PCC, Órfão JJM, Pereira MFR (2004) Adsorption of anionic and cationic dyes on activated carbons with different surface chemistries. Water Res 38:2043–2052

Ferrero F (2007) Dye removal by low cost adsorbents:hazelnut shells in comparison with wood sawdust. J Hazard Mater 142:144–152

Findon A, McKay G, Blair HS (1993) Transport studies for the sorption of copper ions by chitosan. J Environ Sci Health A28:173–85

Forgacs E, Cserhati T, Oros G (2004) Removal of synthetic dyes from wastewaters: a review. Environ Int 30:953–971

Gupta VK, Rastogi A, Dwivedi MK, Mohan D (1997) Process development for the removal of zinc and cadmium from wastewater using slag—a blast furnace waste material. Sep Sci and Tech 32:2883–2912

Gupta VK, Mangla R, Agarwal S (2002) Pb(II) selective potentiometric sensor based on 4-tert-butylcalix[4]arene in PVC matrix. Electroanalysis 14:1127–1132

Gupta VK, Mittal A, Kurup L, Mittal J (2006a) Adsorption of a hazardous dye, erythrosine, over hen feathers. J Colloid Interface Sci 304:52–57

Gupta VK, Mittal A, Gajbe V, Mittal J (2006b) Removal and recovery of the hazardous azo dye acid orange 7 through adsorption over waste materials: bottom ash and de-oiled soya. Ind and Eng Chem Res 45:1446–1453

Gupta VK, Mittal A, Jain R, Mathur M, Sikarwar S (2006c) Adsorption of Safranin-T from wastewater using waste materials-activated carbon and activated rice husks. J Colloid Interface Sci 303:80–86

Gupta VK, Ali I, Saini VK (2007a) Adsorption studies on the removal of Vertigo Blue 49 and Orange DNA13 from aqueous solutions using carbon slurry developed from a waste material. J Colloid Interface Sci 315:87–93

Gupta VK, Jain R, Varshney S (2007b) Electrochemical removal of the hazardous dye Reactofix Red 3 BFN from industrial effluents. J Colloid Interface Sci 312:292–296

Gupta VK, Jain R, Mittal A, Marthur M, Sikarwar S (2007c) Photochemical degradation of the hazardous dye Safranin-T using TiO₂ catalyst. J Colloid Interface Sci 309:464–469

Gupta VK, Ali I, Saini VK (2007d) Defluoridation of wastewaters using waste carbon slurry. Water Res 41:3307–3316

Gupta VK, Jain R, Varshney S (2007e) Removal of Reactofix golden yellow 3 RFN from aqueous solution using wheat husk—an agricultural waste. J Hazard Mater 142:443–448

Gupta VK, Jain R, Varshney S (2007f) Removal of Reactofix golden yellow 3 RFN from aqueous solution using wheat husk—an agricultural waste. J Hazard Mater 142:443–448

Gupta VK, Rastogi A (2008) Equilibrium and kinetic modelling of cadmium(II) biosorption by nonliving algal biomass Oedogonium sp. from aqueous phase. J Hazard Mater 153:759–766

Gupta VK, Ali I (2008) Removal of endosulfan and methoxychlor from water on carbon slurry. Environ Sci Technol 42:766–770

Gupta VK, Rastogi A (2009) Biosorption of hexavalent chromium by raw and acid-treated green alga Oedogonium hatei from aqueous solutions. J Hazard Mater 163:396–402

Gupta VK, Carrott PJM, Carrott MMLR, Suhas (2009a) Low cost adsorbents: growing approach to wastewater treatment—a review. Environ Sci Tech 39:783–842

Gupta VK, Khayat MA, Singh AK, Pal MK (2009b) Nano level detection of Cd(II) using poly(vinyl chloride) based membranes of Schiff bases. Anal Chim Acta 634:36–43

Gupta VK, Goyal RN, Sharma RA (2009c) Novel PVC membrane based alizarin sensor and its application; determination of vanadium, zirconium and molybdenum. Int J Electrochem Sci 4:156–172

Gupta VK, Rastogi A, Nayak A (2010) Adsorption studies on the removal of hexavalent chromium from aqueous solution using a low cost fertilizer industry waste material. J Colloid Interface Sci 342:135–141

Ho YS, McKay G (1999) Pseudo-second order model for sorption processes. Process Biochem 34:451–465

Hoda N, Bayram E, Ayranci E (2006) Kinetic and equilibrium studies on the removal of acid dyes from aqueous solutions by adsorption onto activated carbon cloth. J Hazard Mater 137:344–351

Jain R, Gupta VK, Sikarwar S (2010) Adsorption and desorption studies on hazardous dye Napthol Yellow S. J Hazard Mater 182:749–756

Kargi F, Ozmıhcı S (2005) Comparison of adsorption performances of powdered activated sludge and powdered activated carbon for removal of turquoise blue dyestuff. Process Biochem 40:2539–2544

Lagergren S (1898) Zur theorie der sogenannten adsorption geloster stoffe. Kungliga Svenska Vetenkapsakademiens, Handlingar pp 1–39

Malik PK (2003) Use of activated carbons prepared from sawdust and rice-husk for adsorption of acid dyes: a case study of acid yellow 36. Dyes Pigm 56:239–249

McKay G (1983) The adsorption of dyestuffs from aqueous solution using activated carbon: analytical solution for batch adsorption based on external mass transfer and pore diffusion. Chem Eng J 27:187–196

Mittal A, Mittal J, Malviya A, Gupta VK (2010) Removal and recovery of Chrysoidine Y from aqueous solutions by waste materials. J Colloid Interface Sci 344:497–507

Mukherjee S, Kumar S, Misra AK, Fan M (2007) Removal of phenols from water environment by activated carbon, bagasse ash and wood charcoal. Chem Eng J 129:133–142

Özer A, Dursun G (2007) Removal of methylene blue from aqueous solution by dehydrated wheat bran carbon. J Hazard Mater 146:262–269

Smith JM (1981) Chemical engineering kinetics, 3rd edn. McGraw-Hill, Singapore

Smith JM, Van Ness HC (1987) Introduction to chemical engineering thermodynamics, 4th edn. McGraw-Hill, Singapore

Weber WJ, Morris JC (1963) Kinetics of adsorption on carbon from solution. J Sanit Eng Div Am Soc Civ Eng 89:31–39

Wu FC, Tseng RL, Juang RS (2009) Initial behavior of intraparticle diffusion model used in description of adsorption kinetics. Chem Eng J 153:1–8